Pyrobitumen occurrence and formation in a Cambro–Ordovician sandstone reservoir, Fahud Salt Basin, North Oman

Alain Y. Huc[a], Peter Nederlof[b], Romain Debarre[a], Bernard Carpentier[a], Mohammed Boussafir[c], Fatima Laggoun-Défarge[c], Arnaud Lenail-Chouteau[a] and Nathalie Bordas-Le Floch[a]

[a] Institut Français du Pétrole, Division Geologie-Geochimie, 1 et 4 Avenue de Bois-Préau, 92852, Rueil-Malmaison, France

[b] Petroleum Development of Oman, Oman

[c] Université d'Orléans, UNR 6531 du CNRS, France : *devient en janvier 200 ISTO-UMR6113 CNRS et Université d'Orléans – 45071 Orléans Cédex 2*

Abstract

The Cambro–Ordovician Barik Sandstone reservoirs in the Fahud Salt Basin in Oman contain bitumen which may fill up to 40% of the porosity. In well Jaleel-1, this bitumen was isolated (according to kerogen procedure) and typed by NMR, elemental analysis and density measurements. The isolated bitumen is characterized by: (1) a highly aromatic character (NMR 75% C_{Aro}, H/C atomic ratio: 0.65), (2) a very high sulphur content (4.2%) and (3) a relatively high density (1.3–1.4 g/cm^3). The insolubility and the reflectivity of the bitumen (1.2% Vr) qualify it as a low mature pyrobitumen. The combination of Rock-Eval and density data was used to calculate the actual volume of the pyrobitumen in the rock, as a percentage of porosity. It was found that the pyrobitumen volume shows a negative correlation with total porosity, indicating that small pores are more invaded by bitumen than larger ones. Finally, closed system pyrolysis experiments, performed on oils with different NSO contents, indicate that an in situ oil with a very high content of NSO compounds is required to generate such large amounts of pyrobitumen in the pore system. These observations suggest that the precursor oil of the current pyrobitumen was a very heavy oil tentatively assumed to be the result of a severe biodegradation. Basin modeling shows that the reservoir was charged already in Devonian times. A major uplift brought the oil accumulation near the surface during the Carboniferous and a rather regular burial to the present day position (4500 m, 140°C) (Loosveld et al., 1996). This scenario, involving a residence time at shallow depth, strengthens the biodegradation hypothesis. The numerical modeling, which involves the IFP kinetic model for secondary oil cracking, suggests that pyrobitumen formation is a very recent event. Inclusion of pyrobitumen particles within quartz overgrowth, containing fluid inclusions, provides an upper temperature limit for the beginning of pyrobitumen formation which comforts the result of kinetic modelling.

Author Keywords: Pyrobitumen; Oman; Oil cracking; Biodegradation; Reservoir geochemistry

1. Introduction

The current trend in hydrocarbon exploration to target deep, high temperature prospects has encouraged research on the thermal stability of petroleum. The onset of oil cracking is still a matter of debate but has been predicted for certain oils at temperatures as low as 140°C (Schenk and Horsfield, 1995). The hydrogen mass balance of oil cracking implies that apart from gas, a highly aromatic and insoluble carbonaceous residue, pyrobitumen, is generated. Because deposition of pyrobitumen may significantly deteriorate reservoir quality, bitumen plugging is recognized as a major exploration risk in many hydrocarbon provinces. This is the case of North Oman where bitumen is often identified on routine microscopical examination of thin sections and where several exploration wells have penetrated reservoirs where the porosity is plugged to such an extent that even gas production is impaired.

The purpose of this paper is to investigate the nature and formation of the bitumen occurrences encountered in the Cambro–Ordovician fluvio-deltaic Barik Sandstone reservoirs in the Fahud Salt Basin in Oman.

2. Geological setting

The Jaleel prospect belongs to the Fahud basin which is located on the eastern flank of a north–south graben system. The Fahud basin is separated from the Ghaba salt basin, sited in the central graben itself, by the Makarem-Mabrouk High (Fig. 1 and Fig. 2). The graben system has been emplaced during Infracambrian time, and is coeval with the rifting phases associated with a sinistral motion along the Najd fault which crosses the Arabian plate along a NW–SE direction from Bani Ghayy basins in Saudi Arabia to southern Oman and northern Yemen (Beydoun, 1993). This rifting event was followed by a thermal relaxation, accounting for the development of a Cambro–Ordovician sag basin. The fluvio-deltaic Barik sandstone (belonging to the Andam formation and the Haima Super Group) (Fig. 3) constitutes the reservoir of the Jaleel prospect. It was deposited as a part of the sag fill. During this rift-sag cycle, Infracambrian Huqf source rock intervals were buried to a sufficient depth to generate hydrocarbons (probably during the Ordovician). This rift-sag period was followed by an important phase of uplift starting during Devonian time, probably in relation to the doming which preceded the Gondwana break-up and which caused the erosion/non deposition of most of the Silurian–Carboniferous interval. Finally, the Gondwana break-up itself was achieved during the Permian, thus inducing the creation of the northeastern and southeastern passive margins of the Arabian plate. It results in a renewed subsidence, which was relayed by the creation of a foredeep basin in North Oman, initiated from late Cretaceous, as a consequence of the formation of Oman Mountains and ophiolites obduction. This continuous subsidence has progressively buried the sediments down to their current depth (Beydoun, 1993 and Loosveld et al., 1996).

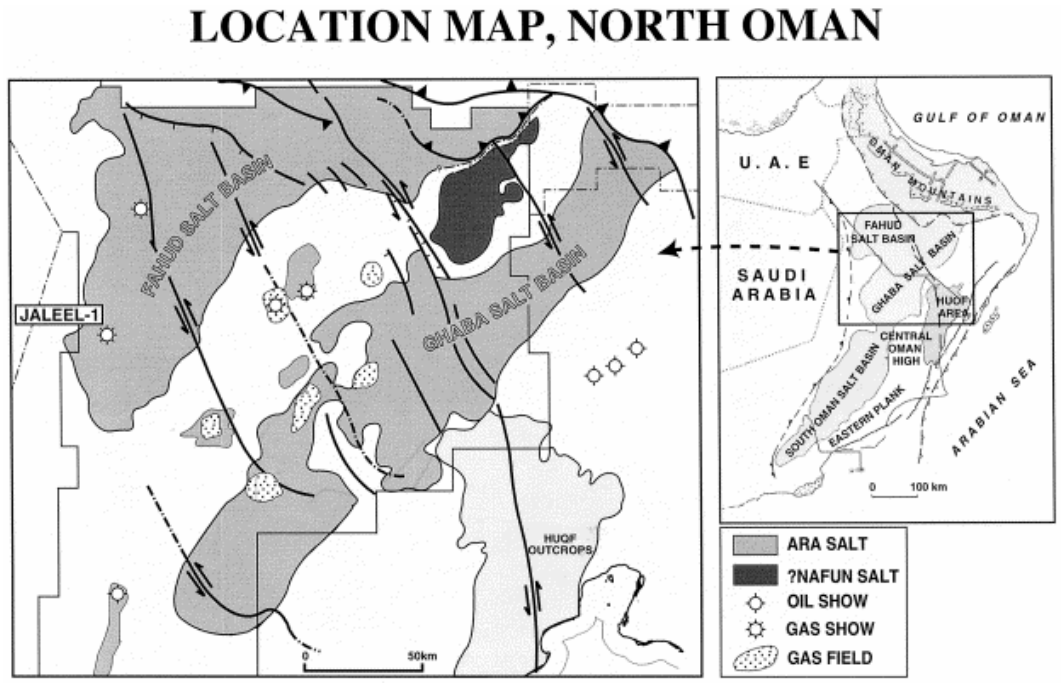

Fig. 1. Location map.

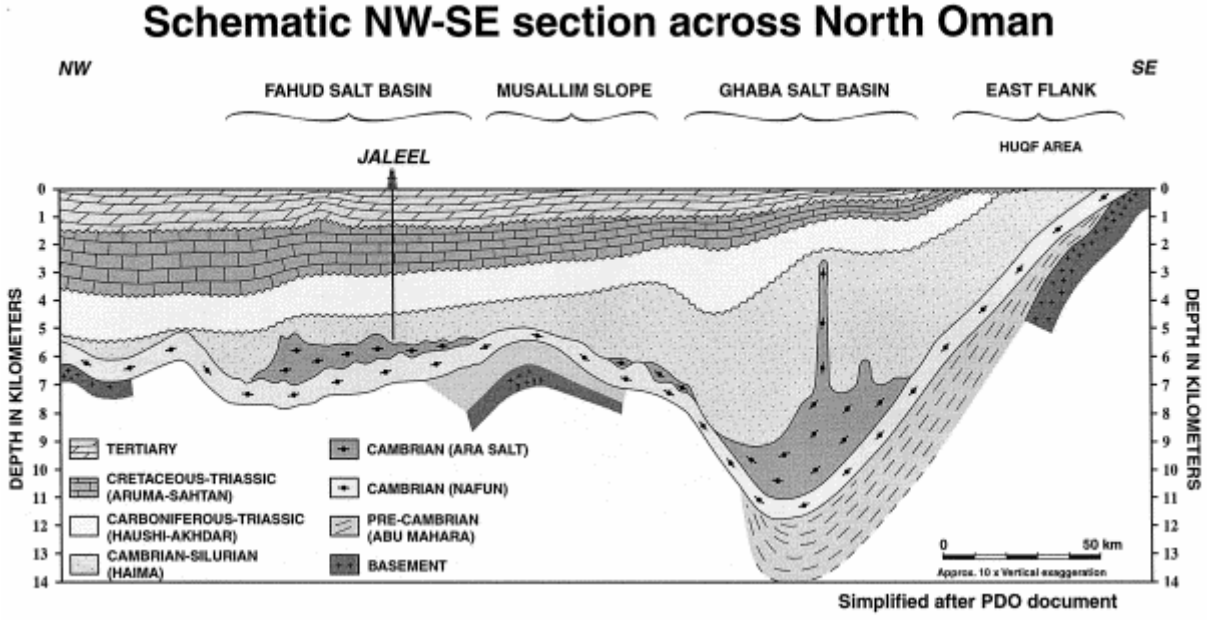

Fig. 2. Schematic NW–SE geological section across North Oman.

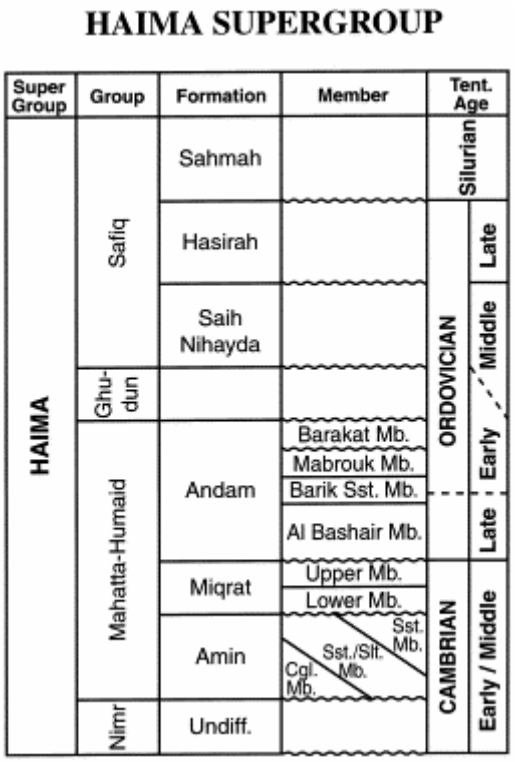

Fig. 3. Stratigraphy of the Haima supergroup.

3. Samples

Twenty-one plugs (JLL1 to JLL21) selected from the 11-m cored section (4560–4571 m) of the Jaleel 1 well were complemented by two cuttings samples respectively assigned to depth intervals: 4480–4560 m (JLLCUT1) and 4571–4636 m (JLLCUT2). As a consequence, the entire set of samples can be considered as representative of a 150-m thick interval of the reservoir. The core samples have been collected at spots where porosity data were available. The two cuttings samples have been separated into two aliquots: one treated as bulk material, the other one, hand picked in order to tentatively sort out different lithological facies.

4. Experimental

Rock-Eval II pyrolysis has been performed on the whole set of samples using the reservoir mode (temperature heating ramp: 10°C/min). Besides the classical S1 peak (light thermovaporizable fraction), this specific mode allows to deconvolute the S2 peak into S2a and S2b peaks which can be respectively assigned to a heavy thermovaporizable fraction and to an actual pyrolyzable fraction (Trabelsi et al., 1994) (Fig. 4). The residual organic carbon is oxidized and the resulting CO_2 is recorded as S4 peak. The total organic carbon (TOC) is calculated from the entire set of generated peaks (Espitalié et al., 1985a; Espitalié et al., 1985b and Espitalié et al., 1985c).

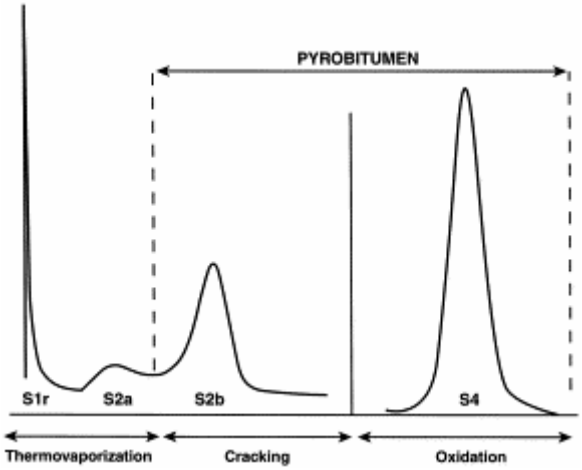

Fig. 4. Rock-Eval pyrogram of a Jaleel rock sample using the "reservoir mode" heating program.

According to the Rock-Eval results, two core samples (JLL15 and JLL17) containing sufficient amount of organic carbon (respectively, 2.3% and 1.5% TOC) have been selected for further characterization of the organic phase.

Visual examination has been performed on these two samples, including microscopical observation of polished sections both in natural light (Plate 1b,c) and UV fluorescence (Plate 1d) and determination of reflectance was made on densimetric concentrates (Plate 1e).

The two selected samples have been subjected to solvent extraction using dichloromethane. The resulting extracts were quantified and, after *n*-heptane deasphalting, separated by thin layer chromatography into saturates, aromatics and NSO fractions. The saturates were then analysed by GC and by GC MS on a VG Autospec; *m*/*z* 191 and *m*/*z* 217 fragmentograms were extracted for comparison with existing regional data base (Grantham et al., 1990).

The insoluble organic matter was isolated following the procedure designed for kerogen preparation involving HF/HCl digestion of the mineral matrix (Durand and Nicaise, 1980).

The resulting organic residue was characterized by elemental analysis including C, H, O, N, S, Fe. The occurring pyrite is evaluated by assuming that the entire Fe is involved as pyrite FeS_2. The sulfur, which is not stoichiometrically associated with the pyrite, is considered to be organic sulfur. The remaining minerals including, in these samples, TiO_2 (anastase), $ZrSiO_4$ (Zircon), $KAlSi_3O_8$ (feldspar microcline), have been tentatively identified by X-ray diffraction supported by X fluorescence which provided the following lists of major elements: S, Zr, Cl, Ca, Ti, Fe, and minor elements: Si, K, V, Ni. ^{13}C solid state ""NMR of the organic residue was performed on a Brucker instrument MSL 400.

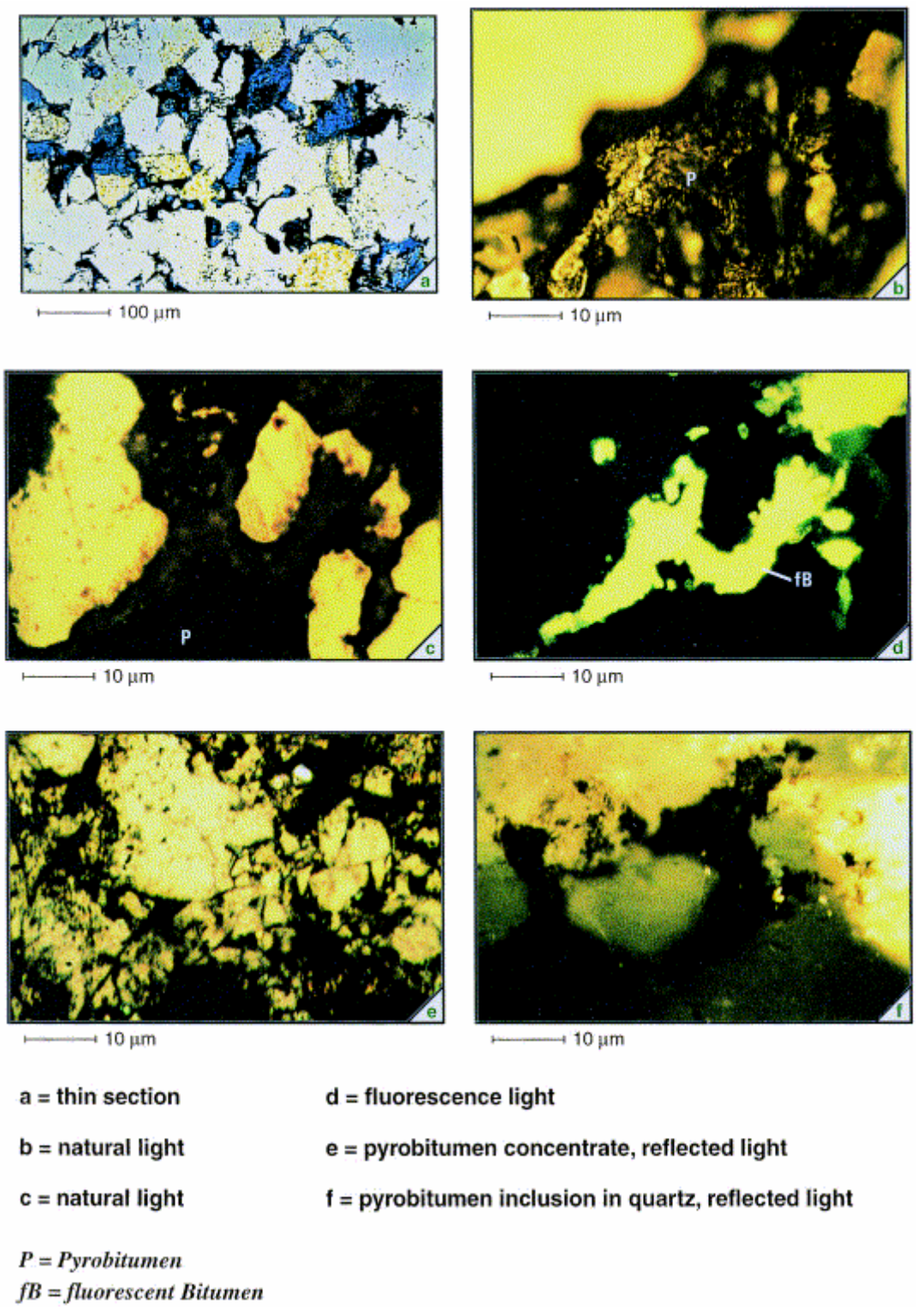

Plate 1. Microphotographs of Jaleel samples: (a) thin section: porosity in blue and pyrobitumen in black; (b) polished section, reflected light: particle of solid bitumen in porosity (quartz in yellow); (c) polished section, reflected light: particle of solid bitumen in porosity (P) and extractable bitumen in brown (see d); (d) polished section, UV light: fluorescent extractable bitumen (fB) corresponding to the brown bitumen in previous microphotograph; (e) polished section, reflected light: particles of solid bitumen resulting from density concentration; (f) polished section, reflected light: pyrobitumen inclusions in quartz.

The density of the organic residue was calculated from its weight (corrected from the estimated pyrite and other minerals weight) and volume (corrected from its Helium porosity and assuming that the volume of the minerals can be neglected).

The stable carbon isotope ratio of the extracts and of the insoluble organic residues was measured using a Delta E Finnigan mass spectrometer, and is reported in the usual δ-notation in units per mil (‰) relative to the Peedee Belemnite standard (PDB).

$$\delta^{13}C(‰)=[(R_{sample}/R_{PDB})-1]\times 10^3$$

where $R=^{13}C/^{12}C$.

5. Results and discussion

5.1. Organic content

According to Fig. 5, the TOC of the 21 core samples ranges from about <0.01wt.% to 2.3 wt.%, although most values are between 0.3 wt.% and 1.2 wt.%, and the average value is 0.7 wt.%.

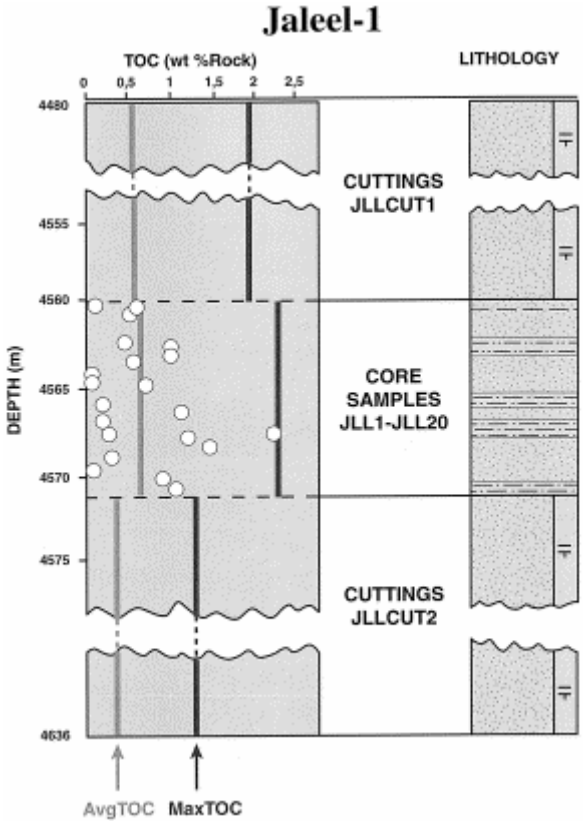

Fig. 5. Total organic carbon (TOC) of the cuttings and core samples.

TOC content of bulk cuttings samples (based on 10 aliquots for each sample), although slightly lower than the core samples average, is comparable to this value: 0.5 wt.% (JLLCUT1) and 0.3 wt.% (JLLCUT2). The TOC content of the hand-picked lithological fractions from JLLCUT1 and JLLCUT2 ranges, respectively, from 0.01wt.% to 1.9 wt.%

(average 0.5 wt.%) and from 0.01wt.% to 1.2 wt.% (average 0.3 wt.%). Moreover, 90% to 95% of the TOC corresponds to refractory nonpyrolysable organic matter, according to Rock-Eval pyrolysis, for the whole set of samples including core and cuttings material, with hydrogen index ranging between 96 and 113. These data suggest that the organic material present in the cored section is rather representative (quantitatively and qualitatively) of the organic matter occurring in the entire considered 150-m thick reservoir interval (Fig. 5).

5.2. Bitumen characterization

Upon solvent extraction, JLL15 and JLL17 core samples release, respectively, 9% and 10% of their carbon as extractable material. The composition of the extracts shown on Table 1 is characterized by its relative richness in saturates.

Table 1. Extract composition

Solvent extract (% extractable carbon)		Carbon isotope ratio of the solvent extract $\delta^{13}C‰$	Saturates % of extract	Aromatics % of extract	Resins % of extract	Asphaltenes % of extract
JLL15	9	−31.9	65.5	10.2	21.4	2.9
JLL17	10	−31.8	73.1	9.8	14.7	2.4

The molecular composition of the extracts, including the significant occurrence of diasteranes, predominance of C27 regular steranes and the abundance of C24 tricyclic terpanes (Fig. 6), together with the isotopic signature of the extracts (Table 1) suggest that they are originating from the regional Q and B source rocks which have been identified by Grantham et al. (1990) and Nederlof et al. (1994) and proposed to be stratigraphically associated with the Ara-salt (at intra and top salt situation).

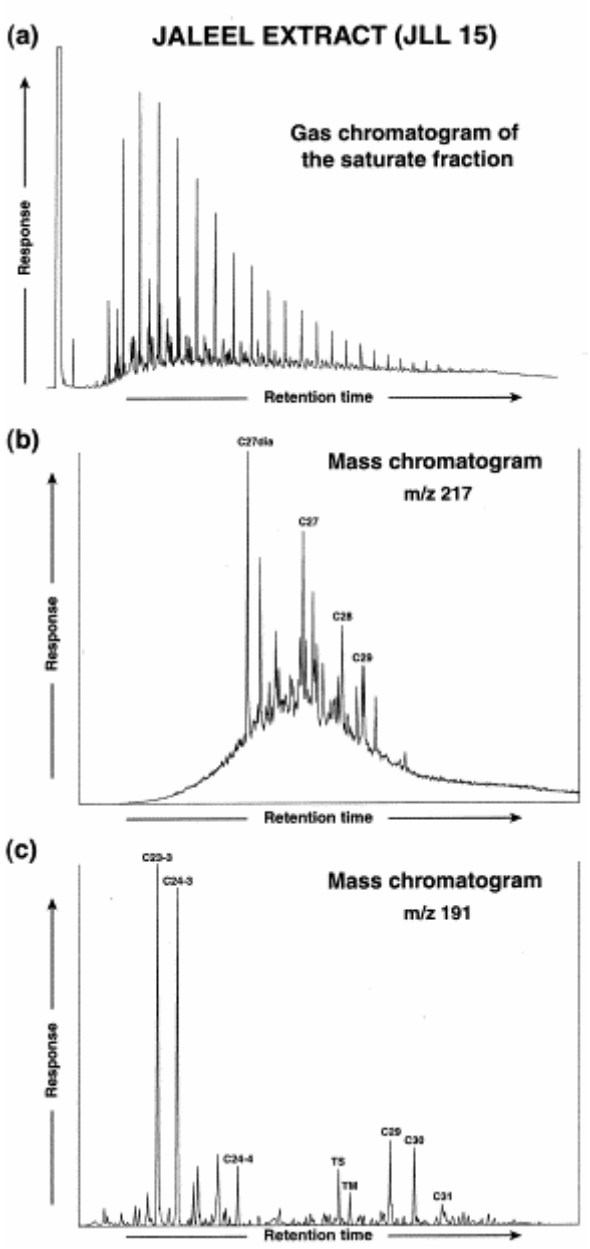

Fig. 6. Gas chromatogram and mass chromatograms (m/z=217 and m/z=191) of a Jalleel rock extract.

5.3. Insoluble bitumen characterization

The elemental analysis of the insoluble organic residue is displayed in Table 2. The samples exhibit an unusually high organic sulfur content (4.14%–4.21%) and a low H/C atomic ratio (0.62–0.64) which reflects a high aromaticity.

Table 2. Elemental and isotopic composition of the insoluble bitumen

	C (wt.%)	H (wt.%)	N (wt.%)	O (wt.%)	Org S (wt.%)	Fe (wt.%)	Pyrite (wt.%)	Other minerals (wt.%)	H/C	O/C ×100	$\delta^{13}C$ (‰)
JLL15	88.16	4.59	0.40	2.72	4.14	0.58	1.24	6.40	0.62	2.31	−35.66
JLL17	87.00	4.67	0.87	3.25	4.21	0.90	1.93	7.03	0.64	2.80	−35.86

A direct measurement of the aromaticity is obtained by ^{13}C solid state NMR analysis (Fig. 7), which reveals that aromatic carbon atoms account for 76%–77% of the total carbon atoms.

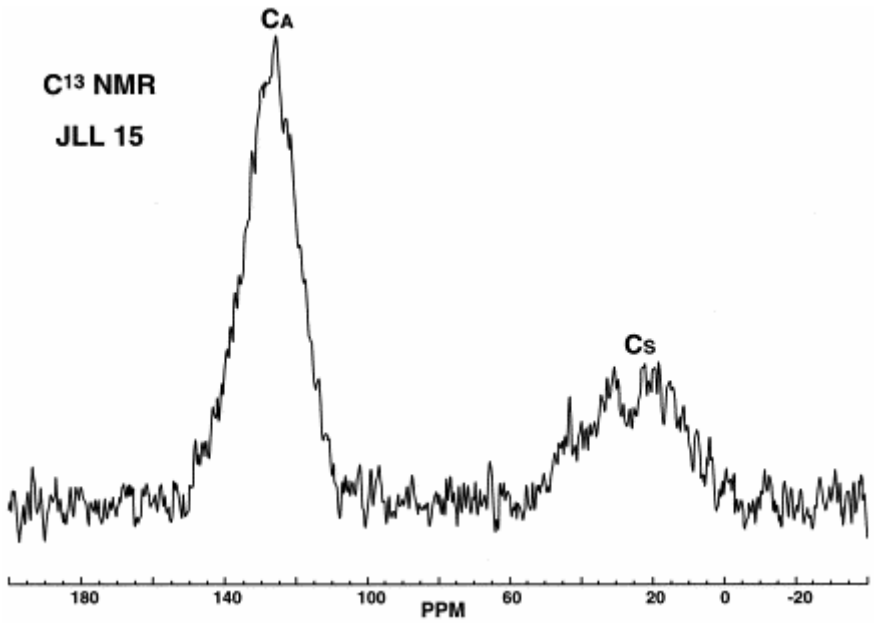

Fig. 7. Solid state 13C NMR of the insoluble bitumen.

The insolubility and the aromaticity of this organic material support its identification as pyrobitumen.

However, the insoluble bitumen reflectance measured on the organic concentrates (Plate 1e) of the two samples (R_o=1.2%) qualifies it as a low maturity pyrobitumen (Hunt, 1995).

The $\delta^{13}C$ of the pyrobitumen is dramatically lower (by 4‰) than the $\delta^{13}C$ of the related extracts (Table 1 and Table 2). This strongly points to a clear difference in origin for the two organic phases which consequently belong to two separate charges of the reservoir, implying a complex filling history. The current gas content of the reservoir potentially represents a third charge, but since no sample of gas has been collected, no analytical evidence can support this assumption. The very light carbon isotope value is characteristic of oils sourced from the so-called Huqf or Nafun infra salt source rock of Precambrian–Infracambrian age. They are probably related to the strong negative excursions of $\delta^{13}C$ which have been recognized worldwide in both organic matter and carbonate within the basal Vendian, uppermost Vendian and early Cambrian (Hsü et al., 1985; Knoll et al., 1986; Magaritz et al., 1986; Kaufman et al., 1991; Burns and Matter, 1993; Narbonne et al., 1994 and Kimura et al., 1997). K–Ar dating and numerical basin modeling (Borgomano, personal communication) indicate that the reservoir was initially charged during the Ordovician and that the "Huqf" source rock located

in the inferred fetch area was generating hydrocarbons at this time. The isotopic identification of the pyrobitumen in the Jaleel prospect clearly indicates that it is a remnant of this early charge of a “Huqf” oil.

5.4. Habitat of pyrobitumen

Microscopical examination of the reservoir rock (Plate 1a,b) shows that the solid bitumen occurs as pore lining and pore filling material. Large particles of nonfluorescent pyrobitumen deteriorate the porosity and are associated with subordinate amount of fluorescing material probably related to the extractable organic matter previously identified. Two silicification events occurred in the reservoir. The first one appears as syntaxial overgrowth around the detrital grains, the other one as autigenic quartz crystals in the pores which reflect the occurrence of a latter diagenetic phase. These autigenic quartz grains are surrounded by bitumen and, locally, particles of pyrobitumen are included in diagenetic quartz (Plate 1f). The homogenization temperatures of the related fluid inclusions indicate that the silicification event took place at a temperature comprised between 130°C and 170°C with a mode at 140°C–145°C (Fig. 8). These temperatures must be compared with the present-day reservoir temperature: 145°C suggesting a recent (ongoing?) phenomenon. These observations imply that the onset of pyrobitumen formation predates at least a part of the silicification event. Most probably the two phenomena occurred concommitantly.

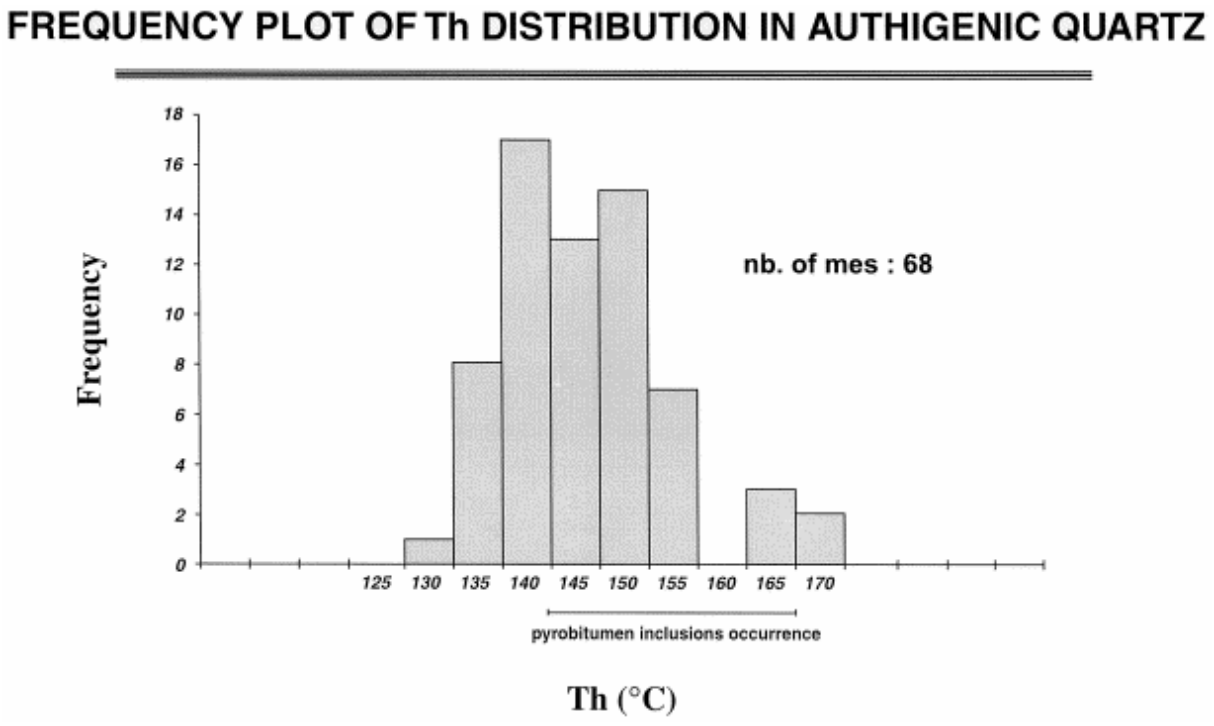

Fig. 8. Histogram of homogenization temperatures of fluid inclusions within quartz inclusions.

In order to evaluate the extent of the pore space alteration, the relative volume of the pyrobitumen within the porosity has been assessed by combining Rock-Eval, porosity, solid bitumen elemental analysis and density data. The Rock-Eval data provide a measurement of the organic carbon content (wt.% TOC) which is converted in wt.% organic matter through the elemental analysis and in vol.% of the porosity (bitumen saturation) through the available petrophysical data and the density of the insoluble bitumen. The latter has been measured to be 1.36 (JLL15) and 1.39 (JLL17). Due to the uncertainty in density determination, resulting from the relatively high mineral content including 1.2%–1.9% pyrite and 6.4%–7% other minerals (Table 2), and the assumption made for density calculation that the volume of ashes is negligible, these values are probably overestimated. Consequently, a conservative density value of 1.3 has been considered for our calculation.

The results of these calculations are displayed in Fig. 9. Fig. 9a shows the positive relationship between the wt.% pyrobitumen and the total porosity (corrected in order to account for both the measured porosity and the porosity occupied by the bitumen) probably reflecting only the fact that the solid bitumen is associated with the porosity. Fig. 9b shows a negative relationship between the bitumen saturation and the total porosity. This latter trend can be tentatively explained by two types of phenomena.

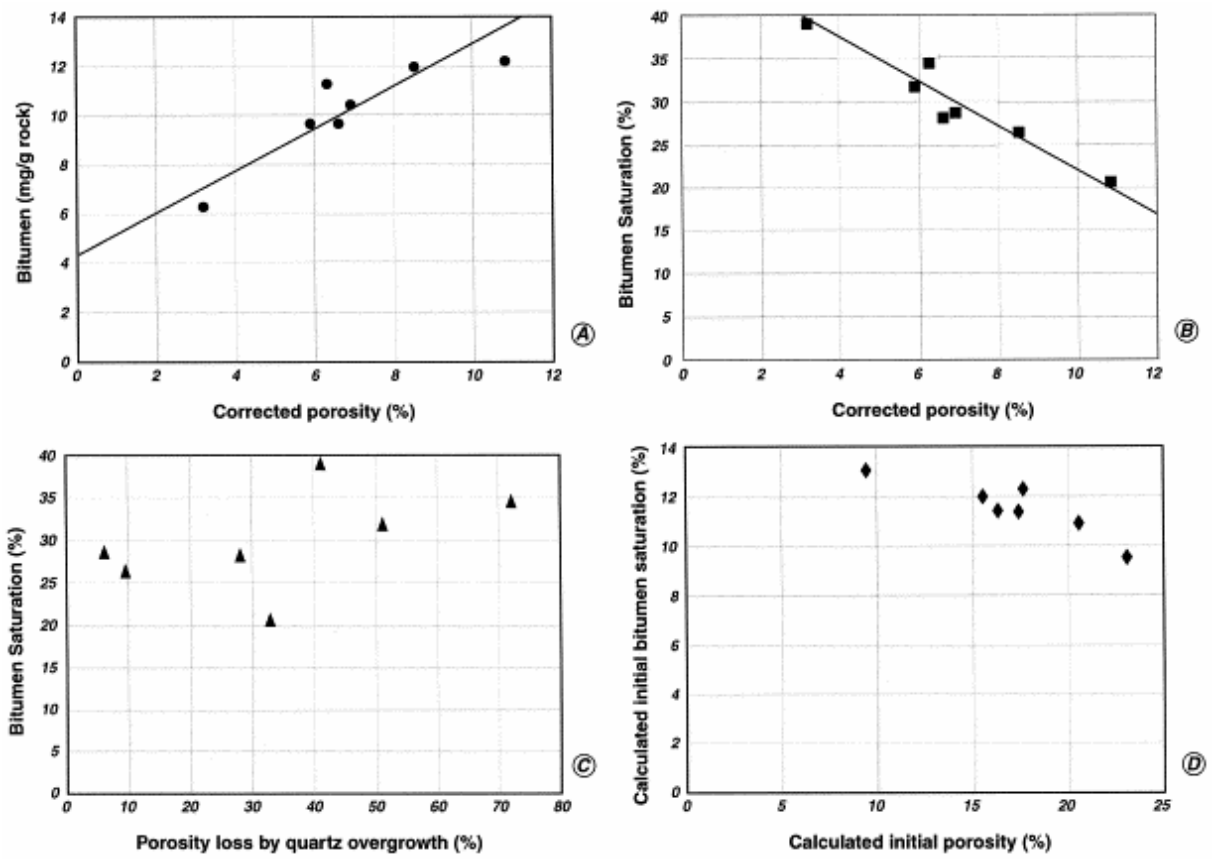

Fig. 9. Relationship between bitumen content and porosity: (a) bitumen (mg/g rock) versus corrected porosity; (b) bitumen saturation (vol.% of porosity) versus corrected porosity; (c) bitumen saturation (vol.% of porosity) versus porosity loss by quartz overgrowth; (d) calculated initial bitumen saturation versus calculated initial porosity.

(a) The relationship is a reflection of various extents of quartz overgrowth differentially reducing the porosity and increasing the relative concentration of bitumen within the porosity. However, according to visual examination of thin sections, the volumetric loss of porosity due to authigenic quartz ranges from 5% to 72% and shows only a very weak correlation with the bitumen saturation (Fig. 9c), implying a subordinate control (if any) of the diagenesis on the observed trend (Fig. 9b). Fig. 9d shows that the pyrobitumen saturation in a diagenetic free reservoir should range between 9% and 13%, which is substantially lower than the 20%–40% observed today but which does not change the unusual importance of the bitumen in the considered samples.

(b) Assuming that the reservoir has experienced several charging steps, the initial Huqf charge might have been better preserved within the lowest porosity from being flushed by subsequent oil charging. As a consequence of the importance of the quartz cementation, this hypothesis is difficult to substantiate. However, it is interesting to note that the observed trend still holds when considering the relationship between the "pre-quartz overgrowth" porosity (calculated by adding the corrected porosity and the estimated porosity lost by quartz cementation) and the "pre-quartz overgrowth" initial bitumen saturation (Fig. 9d).

5.5. Origin of the pyrobitumen

According to laboratory experiments (Behar et al., 1991), the fraction of oil converted to pyrobitumen during the thermal alteration of an oil is related to the initial content in heavy compounds including high molecular weight aromatics, resins and asphaltenes.

In this respect, oil samples from north Oman, including a conventional oil, a biodegraded oil and an asphaltene fraction isolated from the biodegraded oil have been subjected to closed system pyrolysis using the gold tube technology (Behar et al., 1991). The experimental conditions have been set to an isothermal heating at 375°C during 72 h in order to maximize the pyrobitumen yield at the lowest possible temperature. Results are calculated in terms of bitumen saturation in a porosity assumed to be entirely filled up with the initial oil. The amount of generated pyrobitumen is minute for the conventional oil, around 10% of the porosity for the biodegraded oil as starting material, and around 40% for a reconstructed tar sand (based on the data derived from the isolated asphaltenes pyrolysis) (Fig. 10). Assuming that these pyrolysis experiments are representative of the natural thermal alteration of oils, these data suggest that the oil which was originally in the porosity of the Jaleel prospect should have been a very heavy crude oil to account for the observed 20%–40% volume saturation for the existing pyrobitumen. Even if one considers the porosity reduction due the quartz cementation and calculates a pre-quartz overgrowth bitumen saturation, the values are lowered to 9%–13% which are still requiring a heavy oil precursor. Such a heavy crude can occur as a result of the biodegradation of an oil charge affecting the whole reservoir or localized at the OWC, or from the local concentration of NSO compounds within the reservoir due to phenomena such as gravitational segregation or deasphalting.

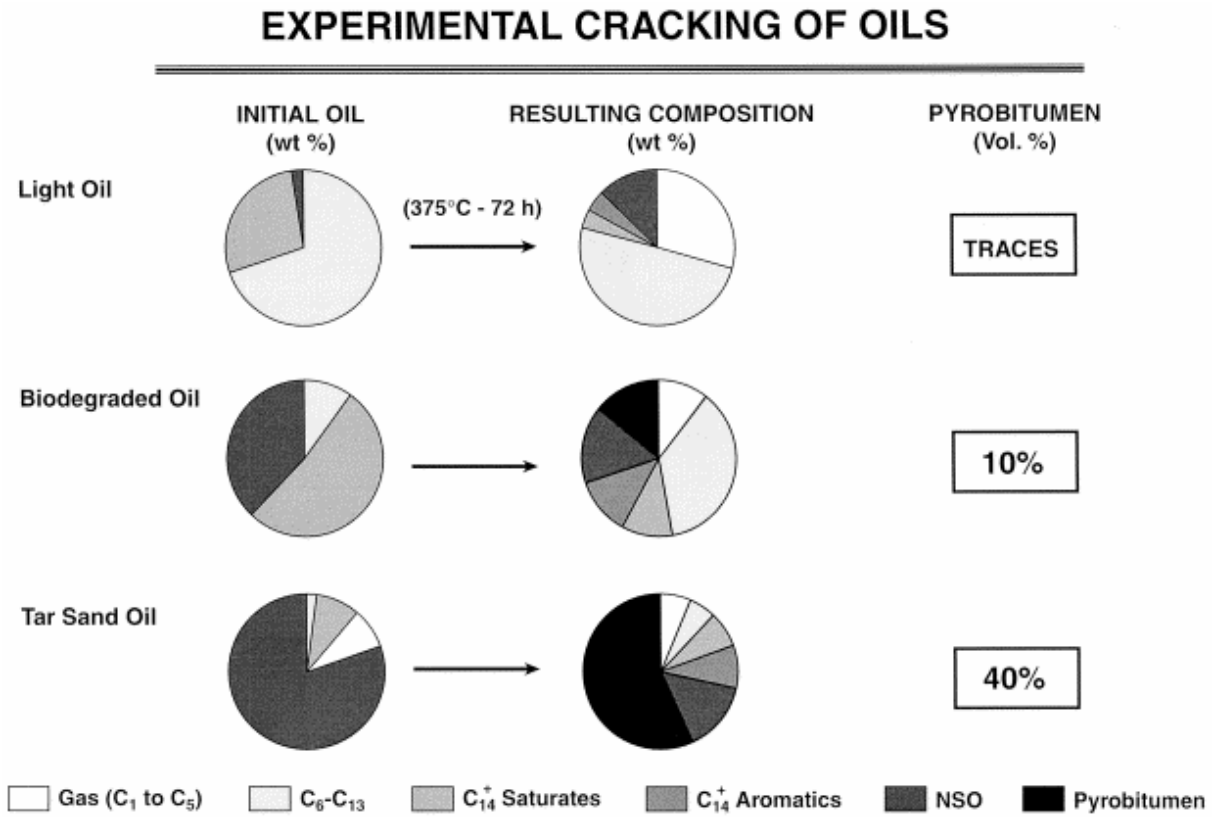

Fig. 10. Experimental cracking of oil: resulting product composition related to initial oil composition.

The fact that the pyrobitumen occurrence affects rather uniformly a 150-m reservoir interval (see above), it precludes situations corresponding to local accumulation of NSO compounds (biodegradation at oil–water contact, deasphalting, gravitational segregation, etc.) and points to a general extensive biodegradation of the initial oil charge. Regional backstriping studies provide a burial history of the Jaleel prospect suggesting an uplift event following the Ordovician charging, bringing the reservoir to a shallow depth during the Carboniferous–Permian time leading to leaching of unstable minerals (e.g., feldspar) (Borgomano, personal communication) probably sufficient for allowing biodegradation to take place. Biodegradation is known to result in sulfur-rich oil (Hunt, 1995). In this respect, the very high sulfur content of the pyrobitumen (>4%) is consistent with such a phenomenon (Table 2).

5.6. Timing of pyrobitumen formation

In order to model the thermal cracking of the oil, we used the kinetic scheme designed by Behar et al. (1992). This model is based on a unique set of cracking reactions for which fixed kinetic parameters have been determined. The only required input is the composition of the initial oil expressed as chemical classes which have been selected by the authors according to molecular weight and thermal stability, and which can be analytically assessed: methane, BTXN (benzene, toluene, xylenes, naphtalenes) and coke are taken as stable, ethane, C3–C5 saturates, C6–C13 saturates, $C14^+$ saturates, C9–C13 aromatics, $C14^+$ aromatics, NSO compounds and precoke are taken as unstable (Behar et al., 1991). In order to account for the formation of pyrobitumen, the latter has been defined as the sum of coke and precoke moieties. The model has been applied without any further adjustment according to the burial history and thermal regime of the Jaleel area (PDO data). As shown in Fig. 11, the considered

initial oil has been taken as a heavily biodegraded crude in order to account for the observed pore saturation. The result of the simulation suggests that the pyrobitumen formation is a rather recent event, probably initiated around 50 million years ago and still in progress (Fig. 11). This is in agreement with the observed relationship between the pyrobitumen particles and the timing of quartz overgrowth constrained by fluid inclusions data.

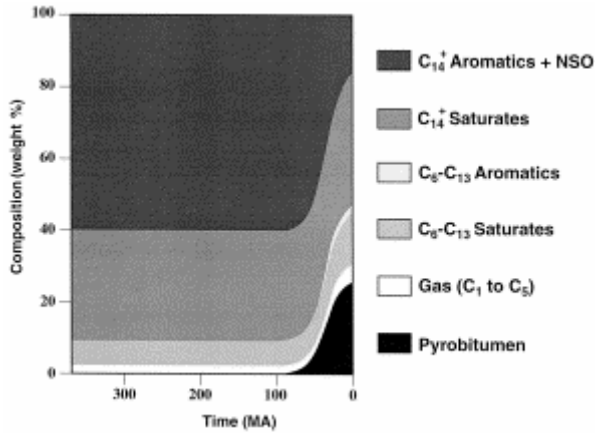

Fig. 11. Numerical modeling of oil composition as a result of natural thermal cracking as a function of time.

6. Conclusion

Based on the available geological and geochemical information, the following scenario is proposed to explain the observed pyrobitumen occurrence in the Jaleel prospect (Fig. 12). Emplacement into the Barik sandstone member of an early charge of oil generated during the Ordovician by a Huqf source rock which was buried as a result of a rifting phase initiated in Infracambrian time. This charging episode was followed by a regional uplift affecting eastern Oman during late Paleozoic and bringing the reservoir to shallow depth where the accumulated oil experienced an extensive biodegradation, resulting in the creation of a very heavy oil deposit (or even in the formation of a tar sand). During the subsequent burial, leading to the present-day depth and associated with the break-up of the Gondwana and the creation of the northeastern and southeastern passive margin of the Arabian plate, this heavy oil deposit underwent a progressive heating increase. This latter thermal history eventually resulted in a secondary cracking process in the last ten million years transforming, by disproportionation reactions, the oil into light hydrocarbons (probably lost) and residual insoluble bitumen. The unusual amount of pyrobitumen is inferred to be a direct consequence of the biodegradation event.

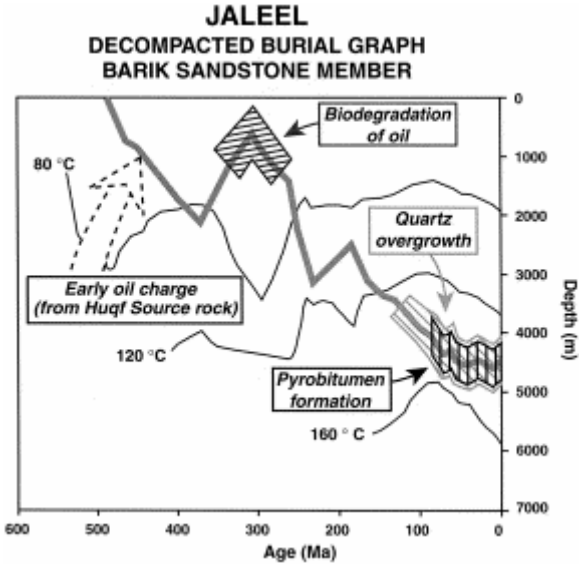

Fig. 12. Proposed scenario for pyrobitumen formation in Jaleel prospect.

The industrial implication of such a scenario is the identification of the two factors controlling the pyrobitumen risk at the regional scale: the charging of the reservoir by a Huqf charge before the regional late-Paleozoic uplift (including timing of source rock maturity and adequate trap structuration) and a sufficient local uplift bringing the considered prospect to a depth allowing the microbial alteration to be effective. Published data indicate that biodegradation can only be significant at a temperature below 80°C (Bernard et al., 1992 and Connan et al., 1997), implying, according to the assumed thermal regime (PDO data) a depth shallower than 1000 m. In this respect, the reconstruction of the burial history of a regional prospect is of prime importance for pyrobitumen prediction.

A more general implication of this study is the validation of the secondary cracking model proposed by Behar et al. (1992). As a matter of fact, the model has been applied without any adjustment. The result of the numerical simulation predicts a timing for the pyrobitumen formation which is perfectly corroborated by the factual data provided by the paragenesis examination. Moreover, the co-occurrence of insoluble pyrobitumen and of saturates containing recognizable biomarkers illustrates the predicted difference of stability between the NSO compounds more readily transformed into solid bitumen and the more stable saturated hydrocarbons.

Acknowledgements

We are indebted to J. Amthor, J. Borgomano, J. Terken, and N. Al-Ruwehy for the fruitful discussions. The used petroleum geology of North Oman is the result of the work of many PDO and Shell Geoscientists, who cannot all be mentioned here. We want to extend our appreciation to the comments made on the first manuscript by J.M. Gaulier, F. Roure and M. Vandenbroucke.

This paper is authorized by the Petroleum Development of Oman LLC and the Ministry of Petroleum and Minerals of Oman. The authors would like to thank the authorities for their permission to publish this paper. This work was supported by the Petroleum Development of Oman.

References

Behar, F., Kressman, S., Rudkiewicz, J.L. and Vandenbroucke, M., 1992. Experimental simulation in a confined system and kinetic modelling of kerogen and oil cracking. *Org. Geochem.* **19** 1–3, pp. 173–189.

Behar, F., Ungerer, P., Kressman, S. and Rudkiewicz, J.L., 1991. Thermal evolution of crude oils in sedimentary basins: experimental simulation in a confined system and kinetic modeling. *Rev. Inst. Franç. Pétrol.* **46** 2, pp. 151–181.

Bernard, F., Connan, J. and Magot, M., 1992. Indigenous microorganisms in connate water of many oil fields: a new tool in exploration and production techniques. In: paper 24811 .

Beydoun, Z.R., 1993. Evolution of the Northeastern Arabian plate margin and shelf: habitat: hydrocarbon habitat and conceptual future potential. *Rev. Inst. Franç. Pétrol.* **48** 4, pp. 311–345.

Burns, S. and Matter, A., 1993. Carbon isotopic record of the latest Proterozoic from Oman. *Eclogae Geol. Helv.* **86**, pp. 595–607.

Connan, J., Lacrampe-Couloume, G. and Magot, M., 1997. Anaerobic biodegradation of petroleum in reservoirs: a widespread phenomenon in nature. In: 18th International Meeting on Organic Geochemistry, Maastricht, The Netherlands, Forschungszentrum Jülich, *Book of Abstracts*, pp. 5–6 Part 1 .

Durand, B. and Nicaise, G., 1980. Procedures for kerogen isolation. In: Durand, B., Editor, , 1980. *Kerogen, Insoluble Organic Matter from Sedimentary RocksTechnip*, pp. 35–53.

Espitalié, J., Deroo, G. and Marquis, F., 1985. La pyrolyse Rock-Eval et ses applications: Part 1. *Rev. Inst. Franç. Pétrol.* **40**, pp. 563–578.

Espitalié, J., Deroo, G. *et al.*, 1985. La pyrolyse Rock-Eval et ses applications: Part 2. *Rev. Inst. Franç. du Pétrol.* **40**, pp. 755–784

Espitalié, J., Deroo, G. *et al.*, 1985. La pyrolyse Rock-Eval et ses applications: Part 3. *Rev. Inst. Franç. du Pétrol.* **41**, pp. 73–89.

Grantham, P.J., Lijmbach, G.W.M. and Posthuma, J., 1990. Geochemistry of crude oils in Oman. In: Brook, J., Editor, , 1990. *Clastic Petroleum Provinces* **50**, pp. 317–328.

Hsü, K.J., Hedi, O., Gao, J.Y., Su, S., Chen, H. and Krahenbuhl, U., 1985. Strangelove ocean before the Cambrian explosion. *Nature* **316**, pp. 809–811.

Hunt, J.M., 1995. In: Freeman, W.H., Editor, , 1995. *Petroleum Geochemistry and Geology*, Freeman, San Francisco 743 pp. .

Kaufman, A.J., Hayes, J.M., Knoll, A.R. and Germs, G.J.B., 1991. Isotopic composition of carbonates and organic carbon from Upper Proterozoic successions in Namibia: stratigraphic variation and the effects of diagenesis and metamorphism. *Precambrian Res.* **49**, pp. 301–327.

Kimura, H., Matsumoto, R., Kakuwa, Y., Hamdi, B. and Zibaseresht, H., 1997. The Vendian–Cambrian d 13C record, North Iran: evidence for overturning of the ocean before the Cambrian explosion. *Earth Planet. Sci. Lett.* **147**, pp. E1–E7.

Knoll, A.R., Hayes, J.M., Kaufman, A.J., Swett, K. and Lambert, I.B., 1986. Secular variation in carbon isotopic ratios from Upper Proterozoic successions of Svalvard and East Greenland. *Nature* **321**, pp. 832–838.

Loosveld, R.J.H., Bell, A. and Terken, J.J.M., 1996. The tectonic evolution of interior Oman. *Geo. Arabia* **1** 1, pp. 28–51.

Magaritz, M., Holster, W.T. and Kirschvink, J.L., 1986. Carbon isotope events across the Precambrian–Cambrian boundary on the Siberian platform. *Nature* **320**, pp. 258–259.

Narbonne, G.M., Kaufman, A.J. and Knoll, A.R., 1994. Integrated chemostratigraphy of the Windermere Supergroup, Northern Canada: implications for Neoproterozoic correlations and early evolution of animals. *GSA Bull.* **106**, pp. 1281–1292.

Nederlof, P.J.R., Gijsen, M.A. and Doyle, M.A., 1994. Application of reservoir geochemistry to field appraisal. In: Al Husseni, M.I., Editor, , 1994. (Gulf Petrolink edn..),*Middle East Petroleum Geosciences GEO 94* **vol. II**, pp. 709–722.

Schenk, H.J. and Horsfield, B., 1995. Simulating the conversion of oil into gas in reservoirs: the influence of frequency factors on kinetic prediction. In: *Selected Papers from the 17th International Meeting on Organic Geochemistry, 4th–8th September, San Sebastian, Spain, A.I.G.O.A.*, pp. 1102–1103.

Trabelsi, K., Espitalié, J. and Huc, A.Y., 1994. Characterization of extra heavy oil and tar deposits by modified pyrolysis methods. In: *Proceedings of the European Symposium on Heavy Oil Technologies in a wider Euro, 7th–8th June, Berlin*, pp. 30–40.